Microbial Detoxification of Superoxide: The Non-Heme Iron Reductive Paradigm for Combating Oxidative Stress

DONALD M. KURTZ, JR.*
Department of Chemistry and Center for Metalloenzyme Studies, University of Georgia, Athens, Georgia 30602

Received April 29, 2004

ABSTRACT
A reductive paradigm has emerged in recent years for detoxification of superoxide and other redox active diatomic molecules in air-sensitive bacteria and archaea. Adventitiously generated superoxide in many anaerobic or microaerophilic bacteria and archaea is scavenged by superoxide reductase (SOR) rather than the classical superoxide dismutases characteristic of aerobic microbes. SORs contain a novel five-coordinate, square-pyramidal [Fe(His)$_4$(Cys)] ferrous active site, which adds a sixth glutamate ligand upon oxidation. This Account summarizes the recently elucidated structural and mechanistic features of SORs. The non-heme iron reductive scavenging paradigm in these air-sensitive microbes also extends to recently characterized enzymes that scavenge hydrogen peroxide and nitric oxide and to oxygen sensing proteins.

Introduction

The toxic side effects of biological electron flow in an aerobic world are well documented. This toxicity stems predominantly from the adventitious one- and two-electron reductions of dioxygen to superoxide and hydrogen peroxide, respectively, and a series of subsequent reactions collectively referred to as oxidative stress.[1] Relatively low steady-state levels of intracellular superoxide (nanomolar) and hydrogen peroxide (micromolar) are sufficient to cause oxidative stress in aerobic bacteria.[2]

Oxidative Stress in Aerobic Bacteria and Archaea. Bacteria and archaea (the microbial "third kingdom of life") are classified as aerobic if they use dioxygen as terminal respiratory electron acceptor and if they also grow optimally under aerobic (as opposed to subaerobic) partial pressures of dioxygen. Aerobic microbes were classically thought to follow what might be termed a disproportionation paradigm for lowering intracellular superoxide and hydrogen peroxide to nonlethal levels.[3] Superoxide dismutases (SODs) catalyze the disproportionation of superoxide to hydrogen peroxide and dioxygen (reaction 1). Most known bacterial SODs contain either non-heme iron or manganese at their active sites.[4] Catalases catalyze disproportionation of hydrogen peroxide to water and molecular oxygen (reaction 2), and the classical catalases contain heme at their active sites.[5] A non-heme, dimanganese-containing catalase has also been described in a few bacteria.[6]

$$2O_2^- + 2H^+ \xrightarrow{\text{SOD}} O_2 + H_2O_2 \quad (1)$$

$$2H_2O_2 \xrightarrow{\text{catalase}} O_2 + 2H_2O \quad (2)$$

Scavenging of lower (micromolar) levels of hydrogen peroxide in many aerobic bacteria, however, occurs predominantly via two-electron reduction to water, reaction 3, catalyzed by peroxidases (hydrogen peroxide reductases). These enzymes typically use one of the reduced pyridine nucleotides, NAD(P)H, as electron donor. Active sites in various aerobic bacterial peroxidases contain hemes or thiols.[7−9]

$$2e^- + 2H^+ + H_2O_2 \xrightarrow{\text{peroxidase}} 2H_2O \quad (3)$$

Oxidative Stress in Air-Sensitive Bacteria and Archaea. Obligately (or strictly) anaerobic bacteria and archaea cannot grow via dioxygenic respiration and usually cannot survive exposure to aerobic levels of dioxygen for extended periods. Nevertheless, many "strictly anaerobic" bacteria and archaea can survive exposure to either air or lower levels of dioxygen for minutes to hours and will resume normal growth upon restoration of an anaerobic environment.[10−13] The sulfate-reducing bacteria are exemplary in this regard. These obligate anaerobes use sulfate rather than dioxygen as the respiratory terminal electron acceptor. The *Desulfovibrio vulgaris* species of sulfate-reducing bacteria not only survives extensive exposure to an aerobic atmosphere,[14,15] it also swims toward and grows optimally near the oxic/anoxic interfaces of sulfate-containing media exposed to air.[16,17] Similar observations have been made on "microaerophilic" bacteria and archaea, which respire dioxygen but grow only under subaerobic partial pressures.[18] Such transiently aerobic or microaerobic growth habitats subject these air-sensitive bacteria and archaea to oxidative stress not only from direct dioxygen inactivation of crucial metabolic enzymes but also from adventitiously produced superoxide and hydrogen peroxide.[2,3] While many anaerobic and microaerophilic bacteria and archaea contain the classical SODs and catalases found in aerobes, many others do not. In *D. vulgaris*, an iron-containing SOD is compartmentalized in the outer periplasmic space, which is separated by a lipid membrane from the inner, much larger cytoplasmic compartment.[14] The cytoplasm of *D. vulgaris* contains no known SOD. Since the negatively charged superoxide cannot readily penetrate membranes

Donald M. Kurtz, Jr., received his Ph.D. degree at Northwestern University with Irving Klotz in 1977 and did postdoctoral work with Richard Holm at Stanford University from 1977 to 1979. He was appointed Assistant Professor of Chemistry at Iowa State University in 1979 and, in 1986, moved to the University of Georgia where he is currently Distinguished Research Professor of Chemistry and Biochemistry & Molecular Biology. From 1987 to 1993, he was an NIH Research Career Development Awardee. His research interests have focused on the structural and functional chemistry and biochemistry of non-heme iron proteins and enzymes, particularly those found in bacteria and archaea that are involved in reactions with dioxygen and its reduction products. More recent investigations of this class of enzymes in the Kurtz lab have included non-heme iron nitric oxide reductases and oxygen sensors.

* Telephone: 706-542-2016. Fax: 706-542-9454. E-mail: kurtz@chem.uga.edu.

10.1021/ar0200091 CCC: $27.50
Published on Web 09/28/2004

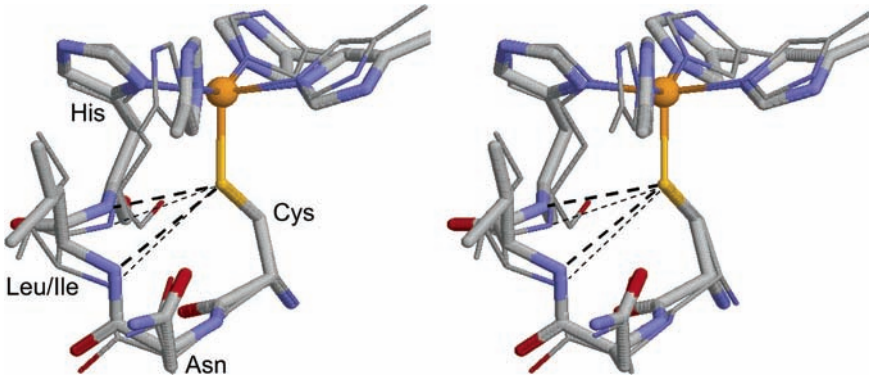

FIGURE 1. Stereoview of the superimposed ferrous SOR active sites from *P. furiosus* 1Fe-SOR[26] (thinner lines) and *D. desulfuricans* 2Fe-SOR[25] (thicker lines). Hydrogen atoms are omitted for clarity. Color coding of atoms is as follows: carbon, gray; nitrogen, blue; oxygen, red; iron, orange; sulfur, yellow. Iron is represented as a sphere; all other atoms are represented in wireframe. N−H···S hydrogen bonds between the peptide backbone and the cysteine sulfur ligand are indicated as dashed lines, and residues comprising the tetrapeptide "chelate" are labeled. (Reprinted or adapted with permission from ref 30. Copyright 2003, Society of Biological Inorganic Chemistry.)

at neutral pH, it can be efficiently scavenged only within the same compartment in which it is generated. This Account focuses on superoxide reductase (SOR), which is cytoplasmic in *D. vulgaris* and in many other air-sensitive bacteria and archaea.[19]

Superoxide Reductases (SORs)

Orientation to SOR Structure and Reactivity. As their name implies, SORs catalyze reaction 4:

$$e^- + O_2^- + 2H^+ \xrightarrow{SOR} H_2O_2 \qquad (4)$$

Historical perspectives on SOR are available elsewhere.[19−24] This Account emphasizes structural and mechanistic aspects of the active site and its relationship to intracellular oxidative stress based on recent results primarily from our laboratory. SORs contain a mononuclear nonheme iron active site, the structure of which is shown in Figure 1.[25,26] The square-pyramidal high-spin "resting" ferrous site with four equatorial histidyl nitrogens and one axial cysteinate sulfur is, so far as is known, unique in biology to SORs and is hereafter referred to as the SOR site. Some SORs contain a second [Fe(SCys)$_4$] site, and we use the acronyms 1Fe-SOR for those containing the site shown in Figure 1 as the only prosthetic group and 2Fe-SOR for those containing the additional [Fe(SCys)$_4$] site. The function of this latter iron site is currently mysterious; at least one 2Fe-SOR remains fully functional when its [Fe(SCys)$_4$] site is removed.[27] SORs are typically isolated with the SOR site predominantly in the ferrous oxidation state, even in air, due to its relatively high ferric/ferrous reduction potential (+200−300 mV vs NHE at pH 7).[19,27,28] The SOR site is thus, not prone to autoxidation, a presumably useful feature in an anaerobic organism suddenly exposed to air. The crystal structures also revealed that in the "resting" ferric state, which is also high-spin, the SOR site contained a sixth monodentate glutamate−carboxylate ligand trans to the cysteinate sulfur.[26]

Kinetics of the Ferrous SOR Site Reaction with Superoxide. The open coordination position trans to the cysteinate sulfur ligand in Figure 1 is an obvious choice for inner sphere reaction of the ferrous site with superoxide, particularly since this site is located at the surface of the protein, is exposed to solvent, but shows no coordinating solvent ligand. Indeed, in 2000, our laboratory in collaboration with that of Diane Cabelli at Brookhaven National Laboratory reported the observation of an intermediate that formed in a second-order, essentially diffusion-controlled reaction between *D. vulgaris* 2Fe-SOR and pulse radiolytically generated superoxide.[29] As shown in Figure 2, this intermediate exhibited an absorption maximum at 590−600 nm ($\epsilon \approx 3500$ M^{-1} cm^{-1}), which was more intense and blue-shifted compared to the spectrum of the resting ferric state (λ_{max} 645 nm, $\epsilon \approx 2000$ M^{-1} cm^{-1}), to which it subsequently decayed in a superoxide-independent, first-order process at 40−50 s^{-1}. As depicted in Scheme 1, we formulated this intermediate as a ferric-peroxo or -hydroperoxo species. The 645-nm absorption of the resting ferric SOR site is due predominantly to π-type CysS$^-$ → Fe(III) charge transfer,[28,30] and this transition should also dominate the absorption of a (hydro)peroxo adduct in the 600-nm region; (hydro)peroxo → ferric charge transfer should make only a very minor contribution.[31] The resting ferrous SOR site shows little or no absorption in the 600-nm region. This initial pulse radiolysis study also showed that an artificially engineered 2Fe-SOR variant, referred to as E47A, in which the glutamate ligand to the ferric SOR site was replaced by a nonligating alanine side chain, gave essentially identical formation and decay kinetics for the 600-nm intermediate to those shown in Scheme 1 at pH 7.7.[29,32] Both the wild-type 2Fe-SOR and the E47A variant lacked significant SOD activity (reaction 1) as measured by pulse radiolysis, implying that removal of the ligating glutamate did not unmask a latent reactivity of the ferric SOR site with superoxide (which would constitute the complementary

Scheme 1

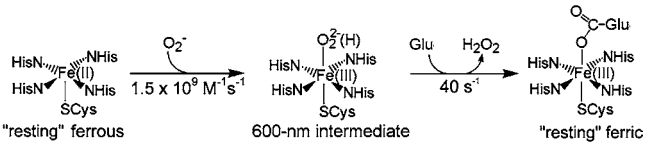

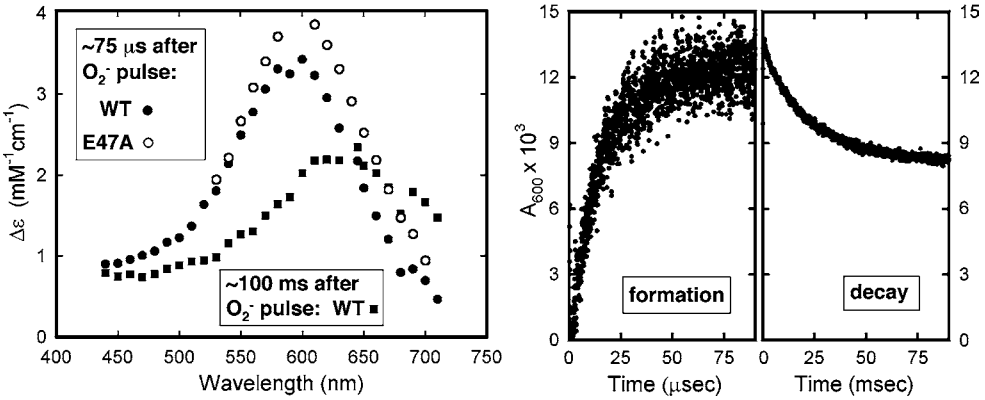

FIGURE 2. Pulse radiolytic detection of an intermediate in the reaction of *D. vulgaris* wild-type 2Fe-SOR (WT) or its E47A variant with superoxide. The left panel shows absorption spectra derived from absorbance time courses such as those shown in the rightmost two panels, which were obtained for the wild-type protein at 600 nm and which show formation and decay of the intermediate. Extinction coefficients in the left panel were calculated assuming stoichiometric (1:1 mol/mol) reaction of superoxide with the SOR site. Conditions were 25−100 μM SOR sites, ~2 μM O_2^- per pulse in 0.12 mM tris(hydroxymethyl)aminomethane, 10 mM formate, 5 μM EDTA, pH 7.8, and 25 °C. (Adapted from ref 29.)

Scheme 2

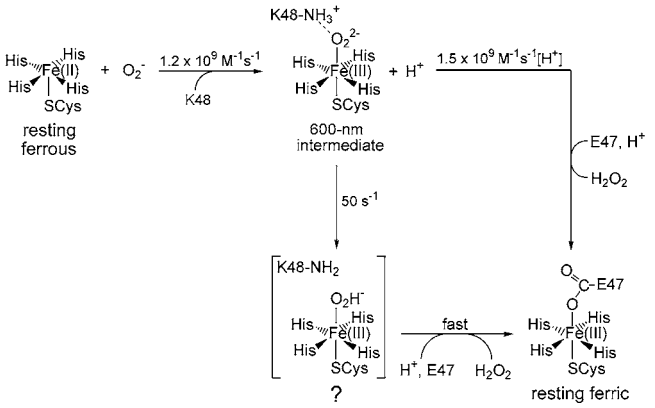

half of a SOD catalytic cycle). Subsequent pulse radiolysis studies detected the same spectroscopic intermediate forming on the same time scale in other 2Fe- and 1Fe-SORs.[19,32,33] The *presumed* inner-sphere electron transfer from the ferrous SOR site to superoxide leading to the ferric-(hydro)peroxo intermediate is consistent with the oxidation of the SOR site by ferricyanide, which results in a cyano-bridged ferrocyanide adduct of the ferric-SOR site.[30,34]

Our subsequent detailed kinetic studies on the *D. vulgaris* 2Fe-SOR led to the elaborated mechanistic scheme shown in Scheme 2.[35] The formulation of the 600-nm intermediate as a ferric-peroxo rather than -hydroperoxo was based on the pH independence of and the lack of a D_2O solvent effect on its essentially diffusion-controlled formation rate and the fact that the same spectroscopic intermediate formed (albeit more slowly) when the proximal residue, Lys48, the side chain of which is a potential proton donor, was changed to an alanine or isoleucine.[32,35] On the other hand, the superoxide anion is strongly hydrogen bonded to solvent in aqueous solution,[36] and if the electron transfer from the ferrous SOR site to superoxide occurs prior to substantial desolvation of the latter (i.e., outer-sphere), then strongly interacting solvent protons could conceivably produce a ferric-hydroperoxo species without a detectable solvent isotope effect.[37] Regardless of whether the 600-nm intermediate is a peroxo or hydroperoxo adduct, the kinetics are consistent with the proximal, positively charged lysyl side chain helping to direct the negatively charged superoxide to the iron site, as suggested from a SOR crystal structure.[26]

Distinct acidic and basic pathways for decay of the 600-nm intermediate were observed. The acidic pathway consists of diffusion-controlled protonation of the intermediate. Above pH 7, a pH-independent decay pathway dominates, which must involve solvent because the decay slows by a factor of 2 in D_2O. The 600-nm intermediate in the E47A variant decayed with a rate constant that was indistinguishable from that of the wild-type SOR in the basic pH range, and we did not detect any subsequent intermediate in either the wild-type or E47A SOR using either pulse radiolysis[35] or stopped-flow mixing.[38,39] The initial decay product must, therefore, be a non-glutamate-ligated species that is rapidly scavenged by E47 to form the resting ferric state. Whether this nonaccumulating decay product is the ferric-hydroperoxo species depicted in brackets in Scheme 2, a five-coordinate ferric site, or a six-coordinate, solvent-ligated ferric site is not known. The E47 side chain may affect decay of the intermediate below pH 7.[35] The rate constants listed in Schemes 1 and 2 apply to *D. vulgaris* 2Fe-SOR measured in our pulse radiolysis studies. For some other SORs, the 600-nm intermediate was reported to decay more rapidly than indicated in Schemes 1 or 2 at pH 7 or above.[19,39,40]

Restrictions on a Ferric-(hydro)peroxo Species at the SOR Active Site. The exact nature of the 600-nm intermediate remains to be established. However, a consideration of the SOR site structure and location within the protein suggests some restrictions on the formation, structure, and reactivity of a ferric-(hydro)peroxo intermediate. The unoccupied sixth ferrous coordination site lies exposed to solvent on the surface of the protein, while the trans cysteinate ligand is shielded from solvent and hydrogen-bonded to two peptide N−H's (cf. Figure 1); these features essentially prevent direct reaction of di-

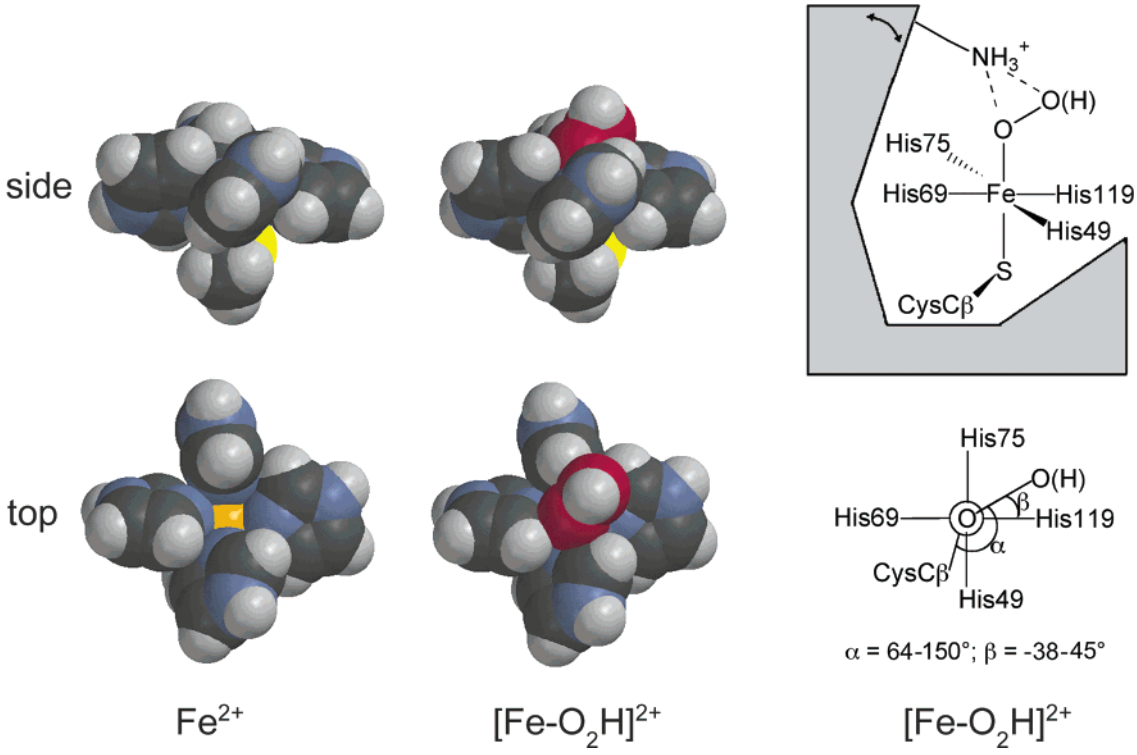

FIGURE 3. Space-filling depictions of DFT-optimized modeled structures of the ferrous SOR site (left) and putative ferric-(hydro)peroxo intermediate (middle) and schematic diagrams showing the geometric restrictions of this intermediate at the SOR site (right). (Adapted from ref 31). The modeled structures used imidazoles and methyl thiolate in place of histidine and cysteine ligands, respectively, and the torsion angles of the imidazole rings around the Fe−N bonds were fixed at those in the *D. desulfuricans* 2Fe-SOR crystal structure.[25] Color coding of atoms is as in Figure 1 except carbon is black and hydrogen is gray.

oxygen species with the cysteine sulfur. The histidine ligand imidazoyl ring planes are sterically restricted to orientations that are considerably out of the average Fe−N_4 plane and these orientations are further restricted by a conserved Cys-Asn-Leu/Ile-His tetrapeptide bidentate "chelate" connecting the cysteine ligand with one of the histidine ligands (cf. Figure 1). As illustrated in Figure 3, the histidine ligands form a pocket above the iron that permits bent ($\angle$Fe−O−O $\approx$ 120°), end-on coordination of the (hydro)peroxo but appears to sterically preclude side-on peroxo coordination (i.e., where both oxygen atoms of the peroxo are coordinated to iron in a triangular geometry) without severe distortion of the coordination sphere, such as breakage of one of the Fe−His bonds.[31] The glutamate-ligated resting ferric SOR site shows no such distortion or appreciable movement of iron toward the carboxylate ligand relative to the ferrous SOR site.[26]

The solvent exposure of the SOR site would facilitate protonation of the iron-bound oxygen of an end-on-coordinated hydroperoxo leading to irreversible Fe−O bond breakage and dissociation of H_2O_2. A potential competing process is double protonation of the terminal oxygen and subsequent heterolytic O−O bond cleavage resulting in a perferryl ($\{Fe(V)=O\}^{3+}$) species, as proposed for the ferric-peroxo at the superficially similar cysteine-ligated heme site of cytochrome P450. This latter process does not appear to occur during the reaction of SOR with superoxide.[31,41] In contrast to the solvent-exposed SOR site, the heme active site of P450 is buried in the interior of the protein, and its reactivity with dioxygen and protons is also substrate-gated, which apparently diverts the chemistry toward perferryl formation. Intrinsic properties of the SOR site may also make P450-type chemistry relatively unlikely. In contrast to the four neutral histidine ligands of the SOR site, the porphyrin ligand in P450 is dinegatively charged, and its highly conjugated electronic structure can delocalize positive charge, both of which would contribute to stabilization of a perferryl. Others have suggested that a low-spin ($S = {}^1/_2$) ferric-(hydro)-peroxo, such as in P450, would be more prone to O−O bond cleavage, whereas a high-spin ($S = {}^5/_2$) ferric-(hydro)peroxo would be more prone to Fe−O bond cleavage.[42,43] The spin state of the 600-nm SOR intermediate is not known. Our DFT calculations indicated that the low-spin ferric-(hydro)peroxo SOR model is more stable than the high-spin state.[31] While we do not discount the possibility of a high-spin SOR intermediate, Kovacs' group has reported that a low-spin, end-on ferric-hydroperoxo species (with a cis rather than trans thiolate ligand) could be produced in methanol from reaction of potassium superoxide with a synthetic five-coordinate ferrous complex.[43,44] This ferric-hydroperoxo species persisted for several minutes at −90 °C but at room-temperature decayed to the ferric ($S = {}^3/_2$) methanol-ligated complex with release of hydrogen peroxide on a time scale similar to that observed for decay of the (presumably) analogous SOR intermediate. A metastable, purportedly side-on, seven-coordinate ferric-peroxo complex of an E47A 2Fe-SOR was reported to form upon reaction of excess hydrogen peroxide with the *ferrous* SOR site.[45,46] This

Scheme 3

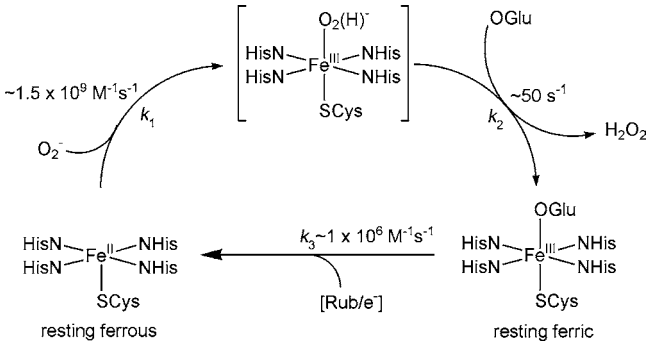

species was reported to persist on a much longer time scale (at least several seconds) than the intermediate resulting from reaction with superoxide (less than 0.1 s), has a different absorption maximum (560 nm) from that of the superoxide-derived intermediates (600 and 620 nm) reported by the same group on the same SOR,[32,40] and leads to degradation of the SOR site. Caution should, therefore, be exercised in inferring that this hydrogen-peroxide-derived species is an intermediate in the SOR catalytic cycle described below.

Completion of the SOR Catalytic Cycle. Rereduction of the ferric SOR site is necessary for completion of the catalytic cycle. To analyze the kinetics of this cycle, we developed the tightly coupled catalytic system diagrammed in Scheme 3, which also serves as a convenient SOR activity assay. This system uses the small electron-transfer protein rubredoxin[47,48] as proximal electron donor to SOR and NADPH as the source of reducing equivalents (which were transferred to rubredoxin via a flavoprotein reductase).[48,49] Xanthine plus xanthine oxidase was used to generate a readily calibrated flux of superoxide.[50] Measurement and analysis of the kinetics of the cycle represented by Scheme 3 showed that 1 μM SOR can convert a 20-μM/min flux of superoxide to a steady-state superoxide concentration of $\sim 10^{-10}$ M, during which any individual SOR site turns over on average about once every 5 s. At such low steady-state concentrations of superoxide, its diffusion-controlled reaction with the ferrous SOR site becomes rate-limiting for turnover. Thus, neither the axial carboxylate ligation (during the k_2 step of Scheme 3) nor deligation (during the k_3 step) limits this turnover. Consistent with this observation, the E47A variant showed activity indistinguishable from that of the wild-type SOR in the catalytic cycle of Scheme 3. The "function" of this ligating carboxylate, thus, remains somewhat mysterious. Cyanide inhibited the SOR turnover but only at high concentrations (20 mM) and only after many hours of preincubation time with the SOR, during which cyanide promotes autoxidation of the ferrous SOR site and formation of the ferric-cyano adduct.[30] This cyanide-ligated SOR site is expected to have a much more negative reduction potential[43] and presumably cannot be reduced on a catalytically competent time scale.

How Do the in Vitro Results Relate To in Vivo SOR Activity? The common laboratory bacterium *Escherichia coli*, which can grow either aerobically or anaerobically, contains no SOR homologues but instead relies on Mn- and Fe-SODs (catalyzing the disproportionation reaction 1) to scavenge superoxide during aerobic growth. As mentioned above and discussed further below, SORs have no significant SOD activity. However, when the heterologous SORs are expressed from plasmids in so-called "SOD-knockout" strains of *E. coli* (which are killed by exposure to air), the intracellular steady-state superoxide is lowered to nonlethal levels by the catalysis of reaction 4 by SOR. The SOD-knockout strain thereby regains the ability to grow aerobically.[14,27,51] This system serves as an in vivo model of how SORs operate in air-sensitive bacteria, as well as a convenient system for testing activities of engineered SOR variants. Since *E. coli* contains no rubredoxin, other unidentified species must serve as proximal electron donors for the intracellular catalysis of reaction 4 by SOR in the SOD-knockout strains. While genetic evidence suggests that rubredoxin is a proximal electron donor to SOR in some organisms,[47,48] the genomes of some SOR-containing microbes do not encode a rubredoxin or rubredoxin-like protein.[51] Furthermore, two other 1Fe-SORs functioned indistinguishably from the 2Fe-SOR in the in vitro cycle described by Scheme 3,[49] and these 1Fe-SORs had also been shown to complement the *E. coli* SOD-knockout strains.[19] SORs, thus, appear to be promiscuous electron acceptors but specific electron donors to superoxide, that is, in times of oxidative stress, SORs efficiently divert intracellular reducing equivalents to scavenge superoxide. Although no estimates are available for air-sensitive microorganisms, 10^{-10} M is near the upper limit of the steady-state superoxide concentration that can be tolerated by aerobically growing *E. coli*.[2,24] Thus, the in vitro turnover cycle shown in Scheme 3 also appears to be a biologically competent model. Since 10^{-10} M is on average less than one molecule per bacterial cell, SOR (like SOD) is a rare example of an enzyme that operates in large excess over its substrate concentration under physiological conditions.

Why Does SOR Not Show Significant SOD Activity? Under the turnover conditions exemplified by Scheme 3, any SOD activity of SOR is unlikely to occur as long as a sufficient supply of reducing equivalents is available to outcompete reduction of the ferric site by superoxide. In fact, the ferric SOR site, even in the E47A variant, shows at most a very sluggish reaction with superoxide compared to the ferrous site, as judged by the low or nonexistent SOD activity of SORs.[23,47] Since reduction of the ferric SOR site by superoxide is thermodynamically highly favorable ($E^{\circ\prime}(O_2/O_2^-) = -0.16$ V vs NHE at pH 7 vs approximately +0.25 V for the ferric/ferrous SOR couple), there must be a significant kinetic barrier to outer-sphere electron transfer, perhaps involving the reorganizational energy required for the change between six- and five-coordination. If facile reduction of the ferric SOR site by superoxide requires inner-sphere coordination, as is proposed for the ferric iron-containing SOD,[4] the low (nanomolar) steady-state concentrations of superoxide generated in the standard SOD assay (or intracellularly) may not be able to compete effectively with the glutamate carboxylate or,

in the case of the E47A variant, with solvent for the ferric SOR coordination site trans to the cysteinate ligand.[40] This explanation is consistent with the low affinities of cyanide and azide for the ferric SOR site, ~10 and ~200 mM of these anions, respectively, being required for saturation in the pH range of 7−9.[28,49] Conversely, at micromolar or higher superoxide concentrations, such as those generated by pulse radiolysis, spontaneous disproportionation of superoxide (~10^5 M^{-1} s^{-1} at pH 8, equivalent to a half-time of <10 s for >1 μM superoxide) must outcompete its reduction of the ferric SOR site.[29] Unlike that of SORs, the "resting" ferric site of the iron-containing SOD is shielded from solvent and five-coordinate,[4] both of which may be more conducive to inner-sphere reaction with superoxide. Reduction of the ferric SOD site by superoxide may also be facilitated by protonation of an ancillary coordinated solvent ligand, a feature that is also absent from the SOR site.

Other Non-Heme Iron Proteins Involved in Microbial Oxidative Stress Protection

So, how does *D. vulgaris* rid itself of the toxic hydrogen peroxide generated by catalysis of reaction 4 by SOR? While *D. vulgaris* was reported to contain a catalase, it has been found to be encoded on a plasmid that is retained by the bacteria only under N_2-fixing conditions; the *D. vulgaris* genome does not encode a recognizable catalase.[15] Furthermore, due to their high K_m's, catalases function efficiently only at millimolar or higher hydrogen peroxide.[2] We have extensively characterized a protein given the trivial name rubrerythrin from *D. vulgaris*, which appears to be among the peroxide reductases (i.e., catalyzing reaction 3) that can efficiently scavenge micromolar levels of hydrogen peroxide in *D. vulgaris* and many other air-sensitive bacteria and archaea.[48,52−54] The hydrogen-peroxide reactive center in rubrerythrin is a non-heme diiron site that superficially resembles, but is distinct from, those of O_2-activating diiron enzymes.[55,56] Microorganisms must also cope with "nitrosative" stress resulting from exposure to either nitric oxide or species derived directly from nitric oxide.[57] A class of non-heme flavo-diiron enzymes that is clearly distinct from the O_2-activating enzymes (and from rubrerythrin) has been shown to reductively scavenge nitric oxide in *E. coli*,[58,59] anaerobic bacteria,[60] and some pathogenic protists (eukaryotic parasites)[61] under anaerobic growth conditions. There is even genetic evidence associating the functions of rubrerythrins, SORs, and the flavo-diiron enzymes in some bacteria.[14,62] A novel membrane-associated hemerythrin-like non-heme diiron protein likely functions as a dioxygen sensor in *D. vulgaris* and other bacteria.[63] Prior to 2000, hemerythrin had been found only in a few marine invertebrates, where it functions as an O_2 storage protein.[64] The active sites in these aforementioned proteins are not iron−sulfur centers, which are found in some bacterial superoxide sensors.[8] A distinctive and divergent set of non-heme, non-sulfur iron enzymes, thus, contributes to detection and reductive scavenging of toxic oxidative diatomic species in air-sensitive microorganisms.

The research described here from my laboratory has been generously supported by the National Institutes of Health. I gratefully acknowledge the essential contributions to this research of Dr. Eric Coulter, Joe Emerson, Radu Silaghi-Dumitrescu, Shi Jin, and Dr. Diane Cabelli.

References

(1) Valentine, J. S.; Wertz, D. L.; Lyons, T. J.; Liou, L. L.; Goto, J. J.; Gralla, E. B. The dark side of dioxygen biochemistry. *Curr. Opin. Chem. Biol.* **1998**, *2*, 253−262.
(2) Imlay, J. A. Pathways of oxidative damage. *Annu. Rev. Microbiol.* **2003**, *57*, 395−418.
(3) Imlay, J. A. How oxygen damages microbes: oxygen tolerance and obligate anaerobiosis. *Adv. Microb. Physiol.* **2002**, *46*, 111−153.
(4) Miller, A.-F. In *Comprehensive Coordination Chemistry II − From Biology to Nanotechnology*; Que, L., Jr., Tolman, W. B., Eds.; Elsevier: Oxford, U.K., 2004; Vol. 8, pp 479−506.
(5) Zámocky, M.; Koller, F. Understanding the structure and function of catalases: clues from molecular evolution and in vitro mutagenesis. *Prog. Biophys. Mol. Biol.* **1999**, *72*, 19−66.
(6) Yoder, D. W.; Hwang, J.; Penner-Hahn, J. E. In *Metal Ions in Biological Systems*; Sigel, A., Sigel, H., Eds.; Marcel-Dekker: New York, 2000; Vol. 37, pp 527−557.
(7) Parsonage, D.; Claiborne, A. Analysis of the kinetic and redox properties of NADH peroxidase C42S and C42A mutants lacking the cysteine-sulfenic acid redox center. *Biochemistry* **1995**, *34*, 435−441.
(8) Carmel-Harel, O.; Storz, G. Roles of the glutathione- and thioredoxin-dependent reduction systems in the *Escherichia coli* and *Saccharomyces cerevisiae* responses to oxidative stress. *Annu. Rev. Microbiol.* **2000**, *54*, 439−461.
(9) Timâoteo, C. G.; Tavares, P.; Goodhew, C. F.; Duarte, L. C.; Jumel, K.; Gâirio, F. M.; Harding, S.; Pettigrew, G. W.; Moura, I. Ca^{2+} and the bacterial peroxidases: the cytochrome *c* peroxidase from *Pseudomonas stutzeri*. *J. Biol. Inorg. Chem.* **2003**, *8*, 29−37.
(10) Rocha, E. R.; Selby, T.; Coleman, J. P.; Smith, C. J. Oxidative stress response in an anaerobe, *Bacteroides fragilis*: a role for catalase in protection against hydrogen peroxide. *J. Bacteriol.* **1996**, *178*, 6895−6903.
(11) Brioukhanov, A.; Netrusov, A.; Sordel, M.; Thauer, R. K.; Shima, S. Protection of *Methanosarcina barkeri* against oxidative stress: identification and characterization of an iron superoxide dismutase. *Arch. Microbiol.* **2000**, *174*, 213−216.
(12) Trinh, S.; Briolat, V.; Reysset, G. Growth response of *Clostridium perfringens* to oxidative stress. *Anaerobe* **2000**, *6*, 233−240.
(13) Karnholz, A.; Küsel, K.; Gossner, A.; Schramm, A.; Drake, H. L. Tolerance and metabolic response of acetogenic bacteria toward oxygen. *Appl. Environ. Microbiol.* **2002**, *68*, 1005−1009.
(14) Lumppio, H. L.; Shenvi, N. V.; Summers, A. O.; Voordouw, G.; Kurtz, D. M., Jr. Rubrerythrin and rubredoxin oxidoreductase in *Desulfovibrio vulgaris*. A novel oxidative stress protection system. *J. Bacteriol.* **2001**, *183*, 101−108.
(15) Fournier, M.; Zhang, Y.; Wildschut, J. D.; Dolla, A.; Voordouw, J. K.; Schriemer, D. C.; Voordouw, G. Function of oxygen resistance proteins in the anaerobic, sulfate-reducing bacterium, *Desulfovibrio vulgaris* Hildenborough. *J. Bacteriol.* **2003**, *185*, 71−79.
(16) Fu, R.; Voordouw, G. Targeted gene-replacement mutagenesis of *dcrA*, encoding an oxygen sensor of the sulfate-reducing bacterium *Desulfovibrio vulgaris* Hildenborough. *Microbiology* **1997**, *143*, 1815−1826.
(17) Eschemann, A.; Kèuhl, M.; Cypionka, H. Aerotaxis in *Desulfovibrio*. *Environ. Microbiol.* **1999**, *1*, 489−494.
(18) Krieg, N. R. Microaerophily and oxygen toxicity. *Annu. Rev. Microbiol.* **1986**, *40*, 107−130.
(19) Abreu, I. A.; Xavier, A. V.; LeGall, J.; Cabelli, D. E.; Teixeira, M. Superoxide scavenging by neelaredoxin: dismutation and reduction activities in anaerobes. *J. Biol. Inorg. Chem.* **2002**, *7*, 668−674.
(20) Kurtz, D. M., Jr.; Coulter, E. D. Bacterial non-heme iron proteins and oxidative stress. *Chemtracts* **2001**, *14*, 407−435.
(21) Kurtz, D. M., Jr.; Coulter, E. D. The mechanism(s) of superoxide reduction by superoxide reductases in vitro and in vivo. *J. Biol. Inorg. Chem.* **2002**, *7*, 653−658.
(22) Adams, M. W. W.; Jenney, F. E., Jr.; Clay, M. D.; Johnson, M. K. Superoxide reductase: fact or fiction? *J. Biol. Inorg. Chem.* **2002**, *7*, 647−652.

(23) Nivière, V.; Fontecave, M. Superoxide reductase: an historical perspective. *J. Biol. Inorg. Chem.* **2004**, *9*, 119−123.
(24) Imlay, J. A. What biological purpose is served by superoxide reductases? *J. Biol. Inorg. Chem.* **2002**, *7*, 659−663.
(25) Coehlo, A. V.; Matias, P.; Fülop, V.; Thomson, A.; Gonzalez, A.; Carrondo, M. A. Desulfoferrodoxin structure determined by MAD phasing and refinement to 1.9-Å reveals a unique combination of a tetrahedral FeS_4 centre with a square pyramidal $FeSN_4$ centre. *J. Biol. Inorg. Chem.* **1997**, *2*, 680−689.
(26) Yeh, A. P.; Hu, Y.; Jenney, F. E., Jr.; Adams, M. W.; Rees, D. C. Structures of the superoxide reductase from *Pyrococcus furiosus* in the oxidized and reduced states. *Biochemistry* **2000**, *39*, 2499−2508.
(27) Emerson, J. P.; Cabelli, D. E.; Kurtz, D. M., Jr. An engineered two-iron superoxide reductase lacking the $[Fe(SCys)_4]$ site retains its catalytic properties in vitro and in vivo. *Proc. Natl. Acad. Sci. U.S.A.* **2003**, *100*, 3802−3807.
(28) Clay, M. D.; Jenney, F. E., Jr.; Hagedoorn, P. L.; George, G. N.; Adams, M. W. W.; Johnson, M. K. Spectroscopic studies of *Pyrococcus furiosus* superoxide reductase: implications for active-site structures and the catalytic mechanism. *J. Am. Chem. Soc.* **2002**, *124*, 788−805.
(29) Coulter, E. D.; Emerson, J. P.; Kurtz, D. M., Jr.; Cabelli, D. E. Superoxide reactivity of rubredoxin oxidoreductase (desulfoferrodoxin) from *Desulfovibrio vulgaris*: a pulse radiolysis study. *J. Am. Chem. Soc.* **2000**, *122*, 11555−11556.
(30) Clay, M. D.; Emerson, J. P.; Coulter, E. D.; Kurtz, D. M., Jr.; Johnson, M. K. Spectroscopic characterization of the $[Fe(His)_4$-(Cys)] site in 2Fe-superoxide reductase from *Desulfovibrio vulgaris*. *J. Biol. Inorg. Chem.* **2003**, *8*, 671−682.
(31) Silaghi-Dumitrescu, R.; Silaghi-Dumitrescu, I.; Coulter, E. D.; Kurtz, D. M., Jr. Computational study of the non-heme iron active site in superoxide reductase and its reaction with superoxide. *Inorg. Chem.* **2003**, *42*, 446−456.
(32) Lombard, M.; Houée-Levin, C.; Touati, D.; Fontecave, M.; Nivière, V. Superoxide Reductase from *Desulfoarculus baarsii*: Reaction Mechanism and Role of Glutamate 47 and Lysine 48 in Catalysis. *Biochemistry* **2001**, *40*, 5032−5040.
(33) Nivière, V.; Lombard, M.; Fontecave, M.; Houée-Levin, C. Pulse radiolysis studies on superoxide reductase from *Treponema pallidum*. *FEBS Lett.* **2001**, *497*, 171−173.
(34) Auchère, F.; Raleiras, P.; Benson, L.; Venyaminov, S. Y.; Tavares, P.; Moura, J. J.; Moura, I.; Rusnak, F. Formation of a stable cyano-bridged dinuclear iron cluster following oxidation of the superoxide reductases from *Treponema pallidum* and *Desulfovibrio vulgaris* with $K_3Fe(CN)_6$. *Inorg. Chem.* **2003**, *42*, 938−940.
(35) Emerson, J. P.; Coulter, E. D.; Cabelli, D. E.; Phillips, R. S.; Kurtz, D. M., Jr. Kinetics and mechanism of superoxide reduction by two-iron superoxide reductase from *Desulfovibrio vulgaris*. *Biochemistry* **2002**, *41*, 4348−4357.
(36) McDowell, M. S.; Espenson, J. H.; Bakac, A. Kinetics of aqueous outer-sphere electron-transfer reactions of superoxide ion. Implications concerning the O_2/O_2^- self-exchange rate constant. *Inorg. Chem.* **1984**, *23*, 2232−2236.
(37) HO_2 is a substantially more powerful oxidant than O_2^-, but with a pK_a of 4.8, HO_2 would constitute only a tiny percentage of total superoxide at pH 9, where the formation rate of the intermediate is the same as that at pH 5.5.
(38) Emerson, J. P. The kinetics and mechanism of superoxide reduction by two-iron superoxide reductase from *Desulfovibrio vulgaris*. Ph.D. Thesis, University of Georgia, Athens, GA, 2003.
(39) Nivière et al. (ref 40) have reported detection of a second chromophoric intermediate using pulse radiolysis on the same *D. vulgaris* 2Fe-SOR where we have reproducibly detected only one intermediate (the ∼600-nm absorbing species) over a wide range of conditions, including removal of the accessory $[Fe(SCys)_4]$ site (refs 27, 35, and 38). The methodological differences that lead to these alternative results are not obvious to us.
(40) Nivière, V.; Asso, M.; Weill, C. O.; Lombard, M.; Guigliarelli, B.; Favaudon, V.; Houée-Levin, C. Superoxide reductase from *Desulfoarculus baarsii*: identification of protonation steps in the enzymatic mechanism. *Biochemistry* **2004**, *43*, 808−818.
(41) Loew, G. H.; Harris, D. L. Theoretical Investigation of the proton assisted pathway to formation of cytochrome P450 compound I. *J. Am. Chem. Soc.* **1998**, *120*, 8941−8948.
(42) Clay, M. D.; Cosper, C. A.; Jenney, F. E., Jr.; Adams, M. W.; Johnson, M. K. Nitric oxide binding at the mononuclear active site of reduced *Pyrococcus furiosus* superoxide reductase. *Proc. Natl. Acad. Sci. U.S.A.* **2003**, *100*, 3796−3801.
(43) Kovacs, J. A. Synthetic analogues of cysteinate-ligated non-heme iron and non-corrinoid cobalt enzymes. *Chem. Rev.* **2004**, *104*, 825−848.
(44) Shearer, J.; Scarrow, R. C.; Kovacs, J. A. Synthetic models for the cysteinate-ligated non-heme iron enzyme superoxide reductase: observation and structural characterization by XAS of an Fe^{III}-OOH intermediate. *J. Am. Chem. Soc.* **2002**, *124*, 11709−11717.
(45) Mathé, C.; Mattioli, T. A.; Horner, O.; Lombard, M.; Latour, J.-M.; Fontecave, M.; Nivière, V. Identification of an iron(III) peroxo species in the active site of superoxide reductase from *Desulfoarculus baarsii*. *J. Am. Chem. Soc.* **2002**, *124*, 4966−4967.
(46) Horner, O.; Mouesca, J. M.; Oddou, J. L.; Jeandey, C.; Nivière, V.; Mattioli, T. A.; Mathé, C.; Fontecave, M.; Maldivi, P.; Bonville, P.; Halfen, J. A.; Latour, J. M. Mössbauer characterization of an unusual high-spin side-on peroxo-Fe^{3+} species in the active site of superoxide reductase from *Desulfoarculus baarsii*. Density functional calculations on related models. *Biochemistry* **2004**, *43*, 8815−8825.
(47) Jenney, F. E., Jr.; Verhagen, M. F. J. M.; Cui, X.; Adams, M. W. W. Anaerobic microbes: oxygen detoxification without superoxide dismutase. *Science* **1999**, *286*, 306−309.
(48) Coulter, E. D.; Kurtz, D. M., Jr. A role for rubredoxin in oxidative stress protection in *Desulfovibrio vulgaris*: catalytic electron transfer to rubrerythrin and two-iron superoxide reductase. *Arch. Biochem. Biophys.* **2001**, *394*, 76−86.
(49) Emerson, J. P.; Coulter, E. D.; Phillips, R. S.; Kurtz, D. M., Jr. Kinetics of the superoxide reductase catalytic cycle. *J. Biol. Chem.* **2003**, *278*, 39662−39668.
(50) Catalase was added to the assay mixtures described by Scheme 3 to scavenge the hydrogen peroxide formed during SOR turnover.
(51) Lombard, M.; Touati, D.; Fontecave, M.; Nivière, V. Superoxide reductase as a unique defense system against superoxide stress in the microaerophile *Treponema pallidum*. *J. Biol. Chem.* **2000**, *275*, 27021−27026.
(52) Coulter, E. D.; Shenvi, N. V.; Kurtz, D. M., Jr. NADH peroxidase activity of rubrerythrin. *Biochem. Biophys. Res. Commun.* **1999**, *255*, 317−323.
(53) Coulter, E. D.; Shenvi, N. V.; Beharry, Z.; Smith, J. J.; Prickril, B. C.; Kurtz, D. M., Jr. Rubrerythrin-catalyzed substrate oxidation by dioxygen and hydrogen peroxide. *Inorg. Chim. Acta* **2000**, *297*, 231−234.
(54) Sztukowska, M.; Bugno, M.; Potempa, J.; Travis, J.; Kurtz, D. M., Jr. Role of rubrerythrin in the oxidative stress response of *Porphyromonas gingivalis*. *Mol. Microbiol.* **2002**, *44*, 479−488.
(55) Jin, S.; Kurtz, D. M., Jr.; Liu, Z.-J.; Rose, J.; Wang, B.-C. X-ray crystal structures of reduced rubrerythrin and its azide adduct: a structure-based mechanism for a non-heme diiron peroxidase. *J. Am. Chem. Soc.* **2002**, *124*, 9845−9855.
(56) Jin, S.; Kurtz, D. M., Jr.; Liu, Z.-J.; Rose, J.; Wang, B.-C. X-ray crystal structure of *Desulfovibrio vulgaris* rubrerythrin with zinc substituted into the $[Fe(SCys)_4]$ site and alternative diiron site structures. *Biochemistry* **2004**, *43*, 3204−3213.
(57) Woodmansee, A. N.; Imlay, J. A. A mechanism by which nitric oxide accelerates the rate of oxidative DNA damage in *Escherichia coli*. *Mol. Microbiol.* **2003**, *49*, 11−22.
(58) Gardner, A. M.; Helmick, R. A.; Gardner, P. R. Flavorubredoxin, an inducible catalyst for nitric oxide reduction and detoxification in *Escherichia coli*. *J. Biol. Chem.* **2002**, *277*, 8172−8177.
(59) Gomes, C. M.; Giuffre, A.; Forte, E.; Vicente, J. B.; Saraiva, L. M.; Brunori, M.; Teixeira, M. A novel type of nitric-oxide reductase. *Escherichia coli* flavorubredoxin. *J. Biol. Chem.* **2002**, *277*, 25273−25276.
(60) Silaghi-Dumitrescu, R.; Coulter, E. D.; Das, A.; Ljungdahl, L. G.; Jameson, G. N.; Huynh, B. H.; Kurtz, D. M., Jr. A flavodiiron protein and high molecular weight rubredoxin from *Moorella thermoacetica* with nitric oxide reductase activity. *Biochemistry* **2003**, *42*, 2806−2815.
(61) Sarti, P.; Fiori, P. L.; Forte, E.; Rappelli, P.; Teixeira, M.; Mastronicola, D.; Sanciu, G.; Giuffrâe, A.; Brunori, M. *Trichomonas vaginalis* degrades nitric oxide and expresses a flavorubredoxin-like protein: a new pathogenic mechanism? *Cell. Mol. Life Sci.* **2004**, *61*, 618−623.
(62) Das, A.; Coulter, E. D.; Kurtz, D. M.; Ljungdahl, L. G. Five-gene cluster in *Clostridium thermoaceticum* consisting of two divergent operons encoding rubredoxin oxidoreductase-rubredoxin and rubrerythrin-type A flavoprotein- high-molecular-weight rubredoxin. *J. Bacteriol.* **2001**, *183*, 1560−1567.
(63) Xiong, J.; Kurtz, D. M., Jr.; Ai, J.; Sanders-Loehr, J. A hemerythrin-like domain in a bacterial chemotaxis protein. *Biochemistry* **2000**, *39*, 5117−5125.
(64) Kurtz, D. M., Jr. In *Comprehensive Coordination Chemistry II − From Biology to Nanotechnology*; Que, L., Jr., Tolman, W. B., Eds.; Elsevier: Oxford, U.K., 2004; Vol. 8, pp 229−260.

AR0200091